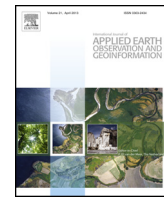




Contents lists available at ScienceDirect

International Journal of Applied Earth Observation and Geoinformation

journal homepage: www.elsevier.com/locate/jag



Estimating temporal changes in soil carbon stocks at ecoregional scale in Madagascar using remote-sensing



C. Grinand^{a,b,*}, G. Le Maire^c, G. Vieilledent^d, H. Razakamanarivo^e, T. Razafimbelo^e, M. Bernoux^a

^a IRD, UMR-Eco&Sols, 2 Place Viala, 34060 Montpellier cedex 2, France

^b Etc Terra, 127 rue d'Avron, Paris, France

^c CIRAD, UMR ECO&SOLS, F-34398 Montpellier, France

^d CIRAD, UPR BSEF, F-34398 Montpellier, France

^e Laboratoire des Radio-Isotopes, Route d'Andraisoro, 101 Antananarivo, Madagascar

ARTICLE INFO

Article history:

Received 4 February 2016

Received in revised form 23 June 2016

Accepted 1 September 2016

Keywords:

Soil organic carbon

Spectroscopy

PLSR

Random forest

Soil-landscape factors

Change detection

Deforestation

ABSTRACT

Soil organic carbon (SOC) plays an important role in climate change regulation notably through release of CO₂ following land use change such as deforestation, but data on stock change levels are lacking. This study aims to empirically assess SOC stocks change between 1991 and 2011 at the landscape scale using easy-to-access spatially-explicit environmental factors. The study area was located in southeast Madagascar, in a region that exhibits very high rate of deforestation and which is characterized by both humid and dry climates. We estimated SOC stock on 0.1 ha plots for 95 different locations in a 43,000 ha reference area covering both dry and humid conditions and representing different land cover including natural forest, cropland, pasture and fallows. We used the Random Forest algorithm to find out the environmental factors explaining the spatial distribution of SOC. We then predicted SOC stocks for two soil layers at 30 cm and 100 cm over a wider area of 395,000 ha. By changing the soil and vegetation indices derived from remote sensing images we were able to produce SOC maps for 1991 and 2011. Those estimates and their related uncertainties were combined in a post-processing step to map estimates of significant SOC variations and we finally compared the SOC change map with published deforestation maps. Results show that the geologic variables, precipitation, temperature, and soil-vegetation status were strong predictors of SOC distribution at regional scale. We estimated an average net loss of 10.7% and 5.2% for the 30 cm and the 100 cm layers respectively for deforested areas in the humid area. Our results also suggest that these losses occur within the first five years following deforestation. No significant variations were observed for the dry region. This study provides new solutions and knowledge for a better integration of soil threats and opportunities in land management policies.

© 2016 Published by Elsevier B.V.

1. Introduction

Soils provide a wide range of ecosystem services including food production, water and climate change regulation but are under pressure from the increasing demands of a growing population (Milne et al., 2014). It is now widely recognized that soil organic carbon (SOC) is critical to most of these services. Restoring, increasing and protecting SOC is therefore a global priority and is covered by the United Nations Conventions on Climate Change, Desertification and Biodiversity (Cowie et al., 2011). Despite global awareness

of climate change and emerging incentives such as reduction of deforestation and forest degradation (REDD+), little is known about soil dynamics associated to changes in land cover and land use. This is especially the case in developing countries that have not set up long term experiments for monitoring soil properties, even though such regions are liable to suffer from major land degradation as a result of deforestation and desertification. Guidelines drawn up by the international scientific community (IPCC, 2006) do not provide any practical means for assessing the complexity and diversity of soil functioning in areas where no inventory has been produced and which do not have any monitoring network (Smith et al., 2012). Practical limitations include the cost of taking soil inventories and the inability to determine the spatio-temporal changes in soil resulting from changes in land use and land manage-

* Corresponding author at: IRD, UMR-Eco&Sols, 2 Place Viala, 34060 Montpellier cedex 2, France.

E-mail address: c.grinand@etcterra.org (C. Grinand).

ment. Spatio-temporal methods using remote sensing technologies provide a means of measuring, monitoring and verifying SOC stocks (Post et al., 2001; Croft et al., 2012; Smith et al., 2012; Minasny et al., 2013).

Given the large amount of carbon stored in the soil worldwide (the top 100 cm soil layer holds 2.5 times more carbon than is found in the Earth's atmosphere, Lal, 2008), a small change in this stock will have a considerable impact on the carbon cycle, by significantly increasing or decreasing the carbon concentration in the atmosphere. The direction and magnitude of changes in SOC stocks are therefore of key importance for climate change policies. The literature generally agrees that conversion from forest to cropland is responsible for the greatest part of greenhouse gas emissions from changes in SOC stocks. There are two main factors: the reduction of input (forest litter vs crop residues) and increase in mineralization of organic matter due to tillage. However, the reduction in SOC stocks given in meta-analysis studies ranges from 42% (Guo and Gifford, 2002), 25% (Don et al., 2011), 15.4% (Powers et al., 2011) to 8.5% (Fujisaki et al., 2015) for forest converted into shifting cultivation or permanent cropland over one or two decades. On the other hand, fallow and pasture tend to increase the SOC stocks with respect to the original forest, by 8% (Guo and Gifford, 2002), 6.8% (Fujisaki et al., 2015), 10% (Powers et al., 2011). It may also lead to a decrease in stocks of up to 12%, as reported in Don et al. (2011). The increase in stocks is explained by changes in root systems that tend to release carbon into the soil and the permanent input from grass or regenerating plant litter. Although these meta-analyses may not be fully comparable as they are based on different criteria for the reference plots (study design, method of calculating stocks, detailed land management, scale, etc.), they highlight the considerable uncertainties in the magnitude and direction of change. For instance, the change in SOC when forest is converted to cropland in Don et al. (2011) ranges from -80% to +58%. Such uncertainty in the direction of change is explained by the complex interaction between the soil and the vegetation, land management methods (e.g. manure management, crop-fallow succession), erosion processes (Croft et al., 2012), climate and soil properties (Guo and Gifford, 2002) and whether the study design is based on a chronosequence or time series (Fujisaki et al., 2015). Most studies of changes in SOC are unrepresentative of tropical landscapes (Powers et al., 2011) and following Smith et al. (2012), "there is an urgent need for development and implementation of higher tier [tiers 2 and 3] methodologies that can be applied at fine spatial scales (e.g. farm/project/plantation)"

Digital Soil Mapping (DSM) has recently emerged as a new soil science discipline with the introduction of new sensors and new statistical techniques (McBratney et al., 2003). DSM sets out to create soil databases at a given resolution by using field and laboratory observation methods coupled with spatial and non-spatial environmental data (covariates) through quantitative relationships (Boenttinger et al., 2010). It has been applied for predicting SOC stocks over a wide range of soils, climates and scales (Minasny et al., 2013). The authors observed that most studies were based on legacy soil data, using internal validation, and that topography, land use/cover and vegetation indices (e.g. NDVI) derived from remotely sensed images were the most widely used covariates. A few studies have been undertaken at field to landscape scale in regions prone to deforestation or soil degradation. Examples include the use of various forms of geostatistics to predict SOC stocks in shifting rain-fed rice cultivation regions in Laos (Phachomphon et al., 2010), the use of regression trees combined with topographic, soil and land use information in eucalyptus growing regions in Madagascar (Razakamanarivo et al., 2011) and the use of Landsat images for smallholder agricultural systems in East African countries (Vagen and Winowiecki, 2013). These studies demonstrate how DSM techniques can be used to estimate SOC stocks at fine scale and at a

given point in time, but they do not predict or assess changes in SOC stocks.

Soil carbon dynamics can be assessed i) using an empirical approach as illustrated above based on a chronosequence or time series to estimate the effect of land use change (Costa et al., 2013), or ii) using a mechanistic model, with various input factors and parameters that describe the ecological processes and make it possible to handle more sophisticated scenarios in the future. These mechanistic models can be associated with spatial information to create a spatially explicit dynamic model (Easter et al., 2007; Milne et al., 2007). However, these models are based on various assumptions or require a large amount of historical input before they can produce accurate predictions of the changes in SOC stocks over a given landscape. Static-empirical or partially dynamic models were described by Minasny et al. (2013) as a mean of producing quick, cost effective estimates of changes in SOC stocks at appropriate land management scales. However, according to these authors, this approach has not yet been explored. The principle is simple and relies on the basic assumption that some soil factors (covariates), such as topography, are stable over time and that others, such as climate or land use, may change with time. By changing the factors in a calibrated SOC spatial model, it is possible i) to predict changes in order to explore various scenarios, and ii) to evaluate stocks retrospectively to create a time series and assess the effect of land use and land management changes on SOC stocks. This study evaluates this pragmatic approach to assessing potential changes in SOC stocks at landscape scale using an easily-accessed environmental dataset and an ad-hoc field soil inventory.

Madagascar is widely recognized for its high level of biodiversity and endemism (Goodman and Benstead, 2005). The biodiversity is mainly found in its remaining natural tropical forests that cover a wide range of climatic conditions (dry, spiny and humid forests and mangroves, cf Fig. 1). In the past 50 years, the area of forest in Madagascar has been reduced significantly (Harper et al., 2007) by traditional slash and burn, pasture extension, charcoal production, illegal logging of precious wood, and mining activities, thus affecting biodiversity, biomass, soil and water resources. Despite well-documented local studies of soil dynamics under various forest and agricultural practices (Vagen et al., 2006; Razakamanarivo et al., 2011; Razafimbelo et al., 2010) and the existence of a national carbon map (Grinand et al., 2009), very little is known about i) the levels and distribution of soil organic carbon at regional scale and ii) the changes in soil organic carbon after deforestation at landscape scale. This paper uses the south-east region of Madagascar as a case study to answer the following questions:

- How are the SOC stocks distributed and what are the underlying drivers?
- Can significant changes in SOC stocks be detected using satellite images?
- How are the estimated changes in SOC stocks linked to land cover and land cover change?

The analysis was based on two soil layers (0–30 cm and 0–100 cm) and two climatic regions (tropical humid and dry) in a region highly prone to deforestation (Grinand et al., 2013), over a twenty years period. The methodology applied involved the following steps: soil inventory, soil analysis and carbon stock calculation, soil-landscape factors collection and preparation, spatial modeling of SOC distribution in 2011, spatial prediction of SOC in 1991, SOC change estimation. We finally compared the SOC change map with published deforestation maps in order to assess SOC change following forest to cropland conversion.

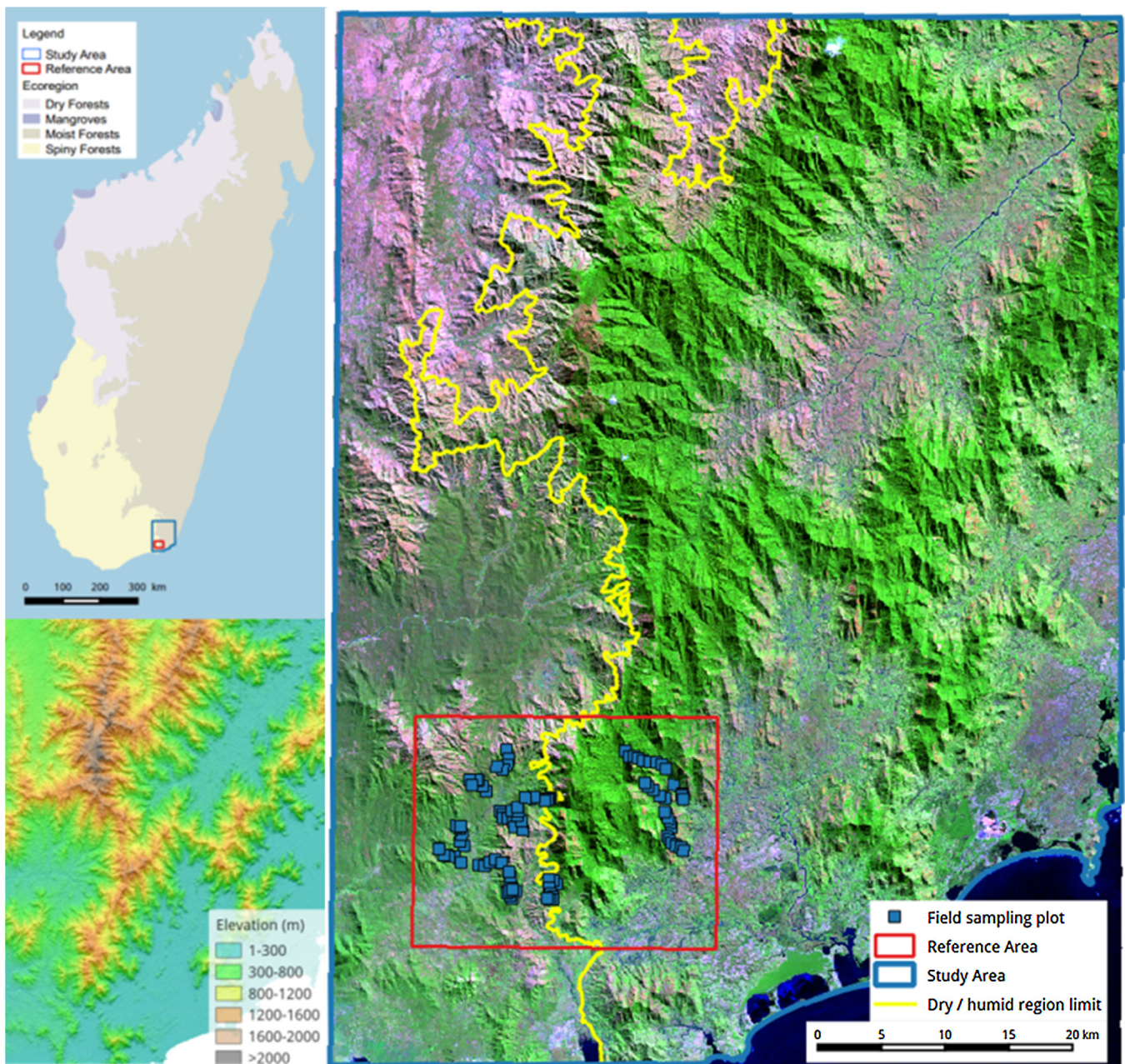


Fig. 1. Location of the study and reference areas with both dry and humid climates. The Landsat image on the right was acquired on July 5 2011. The ecoregion map (top left) was extracted from the Global 200 World Wide Fund project (http://en.wikipedia.org/wiki/Global_200). The boundary between the dry and humid regions (yellow line on map on right) was extracted from (IEFN, 1997). The elevation map (bottom left) was extracted from the ASTER Global Digital Elevation Map (2011). (For interpretation of the references to colour in this figure legend, the reader is referred to the web version of this article.).

2. Material and methods

2.1. Study area

The climate in south east Madagascar is governed by the long south-north ridge that divides the humid mountainous and littoral region to the east and the dry, flat region to the west (Fig. 1), with a narrow transition zone between the two. The boundary between the dry and humid regions is shown in the National Ecological and Forest Inventory (IEFN, 1997) and corresponds to the threshold of around 1000 mm of annual precipitation. The region has acidic basement rocks with dominant ferralsol (54%) in the central and eastern area, acrisol mainly located in the transition zone (10%) and shallow, sandy lithosol (28%) in the dry western area

(Hervieu, 1960). The remaining soils (9%) are calcareous, colluvial and organosol, usually in complex association with the dominant soils in the littoral area.

The area has long been recognized as a major biodiversity hot spot since the creation in 1954 of the Andohahela National Park which has a high level of endemism. It has also been identified as a major hot spot of deforestation in several studies of forest cover changes (MEFT, 2009; Grinand et al., 2013), mainly in the humid region, with an annual natural forest loss rate of about 1%. According to recent statistics, the population density is 30 people per km^{-2} (Vieilledent et al., 2013). Two perimeters were defined: the reference and the study area. The former covers 43 000 ha and was used to calibrate the model. The latter (which includes the reference area) covers 395 000 ha and was used for the spatial/temporal

extrapolation. Both areas show similar biophysical conditions (elevation, climate, Fig. 1).

2.2. Field data collection and soil analysis

2.2.1. Soil inventory

The first step was to collect data and prepare a harmonized dataset of soil carbon stocks for the 0–30 cm and 0–100 cm soil layers. A field survey of 95 10 × 10 m plots on various types of stable land cover (intact forest, crop, pasture) was carried out in 2010 based on topographical transects in the reference area. Soil core samples were taken at four points evenly spaced at 10 m and combined. Five layers (0–10, 10–20, 20–30, 50–60 and 90–100 cm) were sampled. Additional samples were collected to estimate the bulk density of the first three layers, at one corner of the plot and using the cylinder method.

2.2.2. Laboratory and spectral analysis

The samples were taken to the laboratory in Antananarivo (*Laboratoire des Radio-Isotopes*) for analysis. The SOC content of a random selection of 138 samples was analyzed using the wet oxidation method (Wakley Black) and the entire set of samples (n = 440) was scanned using mid infrared spectrometry (MIRS). Spectrometry analysis and chemometric techniques are used routinely to give accurate, cost-effective estimates of many soil properties (Shepherd and Walsh, 2002; Viscarra Rossel et al., 2006) including SOC (McCarty et al., 2002; Grinand et al., 2012) and has already been used in Madagascar (Rabenarivo et al., 2013). Sample reflectance in the mid-IR range was measured between 4000 cm⁻¹ and 400 cm⁻¹ (i.e. 2500 nm and 25,000 nm, respectively) at 3.86 cm⁻¹ intervals with a Nicolet 6700 FT-IR spectrophotometer. Following Rabenarivo et al. (2013) the scan was performed on a 12.6 mm² area of a 0.5 g sub-sample (0.2 mm ground, oven-dried at 40 °C) packed in a well of an 18-well plate. Both spectrum ends were discarded due to noise and only the range 3926–783 cm⁻¹ was considered, yielding 816 data points per spectrum.

2.2.3. Carbon content spectral model

We applied two standards pretreatment procedure (mean average of 5 points followed by Standard Normal Variate transform – SNV) to reduce the noise effect (Viscarra Rossel et al., 2006; Rabenarivo et al., 2013). Then, a local prediction model was developed using partial least square regression (PLSR) available in the “pls” R package based on the 138 laboratory carbon measurement and MIR reflectance. We applied a ten fold cross validation procedure to estimate the optimal number of component (minimum of the root mean square error of prediction – RMSEP) and calculate validation metrics (RMSEP and R²). We obtained a RMSEP of 5.01 g kg⁻¹ and an R² of 0.82 for the cross-validated predictions. The full model was then used to predict the carbon concentration of the 302 samples with no laboratory measurement.

2.2.4. SOC stock calculation for 30 and 100 cm soil layer

A complete soil dataset was obtained for the 0–30 cm soil layer but only sparse estimates for the 0–100 cm layer owing to cost and labor constraints. However, as the carbon content at depth is of great interest because of its large carbon stock and because it can be used for hydrological modeling (Minasny et al., 2013), it was studied in greater detail. Local pedotransfer vertical functions were developed to estimate the bulk density and SOC at unsampled locations in the profile down to 1 m. Splines were used to estimate SOC and rock fragments and linear logarithmic regression as a function of depth was used to estimate the bulk density. This gave estimates at seven points along the vertical profile for each parameter. The vertical profile of each plot was examined visually and five plots

with outlier values were excluded. The harmonized soil dataset and calculated SOC stocks are summarized in Table 1.

2.3. Factors used in the SOC extrapolation model

The second step was to collect and define relevant spatial predictors of SOC stock distribution. There is a well established group of soil-landscape factors that are commonly used in DSM applications (McBratney et al., 2003; Grunwald, 2009). A set of 20 soil-landscape factors was compiled (Table 2) from easily-accessed sources.

A freely available Landsat image (<http://usgs.earthexplorer.org>), acquired on June 5, 2011, was selected because of i) its date that was close to the inventory date, ii) it is available as a Global Land Survey (GLS) product (Gutman et al., 2005) which are made of composite of Landsat TM and ETM+ and iii) the cloud cover was delimited and low. A second GLS image acquired on July 24, 1991 was used for extrapolation into the past (see 2.5). The datasets have the reflectance of the land surface in the visible and near infra-red regions which is widely used to indicate the primary and ecological productivity. The reflectance in the middle and thermal infrared bands depends mostly on the soil properties (Mulder et al., 2011; Croft et al., 2012).

Local geomorphological factors were derived at 30 m resolution from the ASTER Global Digital Elevation Map (2011) using standard Geographical Information System (GIS) software (QGis, SAGA and Grass). These factors describe the physical landscape (slope, aspect, convexity) and represent ecological processes such as potential water storage downslope (wetness index), erosion potential (length of slope) and insolation.

Two climatic factors, annual precipitation and mean annual temperature, were added from the WorldClim database (Hijmans et al., 2005) as they are known to influence soil carbon distribution and soil carbon change after land use change (Guo and Gifford, 2002) and gamma radiometric datasets were obtained from the Ministry of Energy and Mines and explore the potential of K, U and Th relative concentration in explaining SOC stock distribution. Gamma radiometrics provide useful information for soil organic mapping, as a proxy of water retention and clay content (Rawlins et al., 2009) and even more interestingly for characterising erosional, depositional and weathering processes (Wilford and Minty, 2006). From these datasets, the concentrations of potassium (K), uranium (U) and thorium (Th) were selected as factors. These datasets are at 100 m resolution. Given that spatial factors have a wide range of ground resolutions and that the aim was to detect SOC stock change from field scale upwards, a working grid of 30 m was used. Climatic factors were fitted to the 30 m grid by using cubic splines interpolation and the gamma radiometric dataset factors were resampled using the nearest neighbors technique.

2.4. Calibration of the SOC spatial model

The next step aimed to build a multivariate model to explain the spatial distribution of SOC as a function of the covariates. Firstly, a zone of 10 m around the center point of the plot was used to represent the ground sampling location. These zones were intersected with the 30 m spatial covariate grid, creating a total of 195 data points for the calibration dataset, as some plots intersected more than one of the 30 m grid cells. Then, an ensemble machine learning approach was applied using the “Random Forests” algorithm (Breiman, 2001). This algorithm has been shown to be useful for complex and non-linear ecological applications such as soil organic carbon mapping (Grimm et al., 2008; Vagen and Winowiecki, 2013; Screenivas et al., 2014; Wiesmeier et al., 2011) and above-ground biomass mapping (Le Maire et al., 2011a; Baccini et al., 2012; Asner et al., 2012; Vieilledent et al., 2016). A 10 fold cross validation procedure was applied to evaluate the means and standard

Table 1

Soil inventory summary statistics. n represent the number of soil samples for the three soil variables and number of plots for SOC 30 (soil organic carbon stocks for the top 30 cm soil layer) and SOC 100 (soil organic carbon stocks for the top 100 cm soil layer). Min. minimum, max, maximum, s.d. standard deviation.

Climate region	Soil variable	Unit	n	mean	min	max	s.d.
dry	bulk density	g.cm ⁻³	314	1.0	0.7	1.2	0.1
	coarse fragment	%	314	12.0	0.0	39.9	7.1
	organic carbon	g.kg ⁻¹	314	10.8	2.2	47.0	8.3
	SOC30	Mg.C.ha ⁻¹	45	38.0	12.6	72.1	15.4
	SOC100	Mg.C.ha ⁻¹	45	80.5	35.2	141.1	27.2
humid	bulk density	g.cm ⁻³	315	1.0	0.7	1.2	0.1
	coarse fragment	%	315	5.0	0.0	20.7	4.5
	organic carbon	g.kg ⁻¹	315	17.7	2.3	87.3	14.4
	SOC30	Mg.C.ha ⁻¹	45	69.2	37.7	131.1	25.4
	SOC100	Mg.C.ha ⁻¹	45	135.5	75.1	210.5	37.9

Table 2

Spatial soil factor database and results of correlation with SOC stocks for 0–30 cm (SOC30) and 0–100 cm (SOC100) soil layers.

Category	Soil-Landscape factor	Name	Unit	Correlation		
				SOC30	SOC100	
Soil & Vegetation	Landsat band 1 (blue)	B1	reflectance	-0.47	a	-0.39
	Landsat band 2 (green)	B2	reflectance	-0.42	a	-0.34
	Landsat band 3 (red)	B3	reflectance	-0.41	a	-0.35
	Landsat band 4 (near infra red)	B4	reflectance	-0.07		-0.01
	Landsat band 5 (middle infra red)	B5	reflectance	-0.37	a	-0.29
	Landsat band 6 (thermal infra red)	B6	reflectance	-0.25	a	-0.20
	Landsat band 7 (middle infra red)	B7	reflectance	-0.38	a	-0.31
Geomorphology	Elevation	ALT	meter	0.35	a	0.27
	Slope	SLP	degree	0.21	a	0.19
	Aspect	ASP	degree	-0.02		-0.07
	Valley depth	VAH	meter	0.35	a	0.37
	Ridge height	RID	meter	0.20	a	0.14
	Topographic wetness index	TWI	–	0.11		0.13
	Insolation	NRJ	watt.m ⁻²	-0.24	a	-0.30
Climate	Length of the slope	LS	meter	0.27	a	0.26
	Mean annual precipitation	MAP	meter	0.47	a	0.50
Parental material	Mean annual temperature	MAT	°C	-0.48	a	-0.41
	Potassium	K	–	0.07		0.02
	Uranium	U	–	0.04		-0.05
	Thorium	TH	–	0.20	a	0.14

^a indicates that the p-value (Pearson's test) is less than 0.01 for the correlation between the landscape factor and the SOC stock value.

deviations. Standard regression quality indices, root mean square error (RMSE, absolute and in% relative to the mean) and R², bias and ratio of performance to deviation (RPD) were produced for the cross-validation dataset. This validation procedure appeared to be a good compromise for providing realistic values between optimistic methods such as the out-of-the-bag, leave-one-out and standalone test-set procedures and difficult to achieve, external or geographically distant validation approaches, which were not possible in this case. This procedure was already used in other digital soil mapping studies (Grimm et al., 2008; Razakamanarivo et al., 2011). Further calibration tests were performed including change of covariates dataset and change in randomForest parameters (*mtry*, *ntree*). The former was based on our expert local knowledge and the result of the relative importance of the factor measured by the randomForests algorithm (*NodePurity*). *NodePurity* is an importance index calculated by random Forest, that measure the change in residual sum of squares from splitting on the variable, averaged over all trees. Several linear models were compared with the random forest model using the same validation procedure, but these always produced poorer results (data not shown). All statistical tasks described above and below were performed using R-statistics version 3.02 (R Development Core Team, 2005), the randomForest package version 4.6–10 (Liaw and Wiener, 2014) and raster package version 2.3–40 (Hijmans et al., 2015).

2.5. Spatial prediction over the study area

Once the model had been calibrated for the reference area (43,000 ha), it was applied to predict the SOC over the entire study area (395,000 ha). This involved considering the representativeness of the reference area (Lagacherie et al., 2001) and the applicability of the model, with a known level of accuracy, at cell scale (Grinand et al., 2008). There is potentially many source of uncertainty: i) in the calculation of SOC stocks, such as sampling errors (e.g. depth), laboratory analysis, pedotransfer functions (Goidts et al., 2009), and ii) in the spatial modeling, such as approximations for the raw covariates (e.g. slope derived from 30 m GDEM, geometrical distortion of the satellite image) and standard errors of the model parameters and residuals. Considerable effort is required to take into account all sources of uncertainty, using error propagation techniques, which rely on assumptions for estimating the accuracy at cell level. This study used model averaging techniques to estimate accuracy at cell level. This implied producing 10 carbon maps using 10 different models set using a random bootstrap selection of 70% of the calibration dataset. This technique has been applied in previous works on biomass mapping (Casey et al., 2012) and is considered to provide an integrated estimate of the uncertainty from both sampling and modeling. Finally, the carbon maps were combined to produce the mean (SOC_{mean-2011}) and standard deviation (SOC_{sd-2011}) from the 10 bootstrap maps.

2.6. Prediction of SOC stocks in 1991

In the final step, the covariates were split into stable and dynamic sets. Over the 20 year analysis period, only the soil-vegetation covariates ([Table 2](#)) derived from Landsat images were considered to be dynamic. The Landsat image acquired on July 24, 1991 was selected using the same geometrical and cloud cover criteria as for the 2011 image. The 1991 image could not be used directly since reflectance changes may arise from atmospheric conditions, sensor properties or acquisition geometry, and not from changes in soil-vegetation status. These image-related changes apply to the entire image, which was confirmed in this case by pairwise band comparison, revealing small reflectance variations in the overall image statistics (min, max, standard deviation, quantile). Invariant target detection is a simple method used to correct for these changes. Some pixels are considered to have constant characteristics over time, and so changes in their reflectance observed from satellites is considered to come from the atmosphere, geometry of acquisition, and sensor properties. If there are a number of these invariant pixels, a correction equation can be calibrated, which is generally linear (gain, offset) ([El Hajj et al., 2008](#)). In this case, no clear invariant targets were found, and so it was decided to use all the points in the images, as described by [Le Maire et al. \(2011b\)](#), assuming that i) acquisition-related changes affect the entire image, ii) a large majority of the pixels will not have large intrinsic reflectance changes (even if not totally “invariant”). The correction procedure simplified to the calibration of a band-specific linear regression between the 1991 and 2011 images, followed to the application of the obtained gain and offset. To ensure the robustness of this regression, pixel-to-pixel regressions were checked to ensure that they gave the same gain and offset parameters for different pixel resolutions (results not shown). The SOC stock distribution in 1991 was then predicted by applying the same procedure and model as for 2011 (previous [Section 2.5](#)), i.e. using bootstrap model averaging to produce mean ($SOC_{mean-1991}$) and standard deviation ($SOC_{sd-1991}$) maps.

2.7. Detection of changes in soil carbon stocks

Potential SOC stock change maps ($SOC_{1991-2011}$) were produced by subtracting $SOC_{mean-1991}$ from $SOC_{mean-2011}$, and dividing by $SOC_{mean-1991}$ to determine the relative change ($SOC_{1991-2011}\%$). However, maps of SOC stock changes (0–30 cm and 0–100 cm soil layers) included errors from the two carbon maps which needed to be removed before significant SOC changes can be determined. Three post-processing steps were carried out. To address extrapolation issues, thresholds on minimum and maximum reflectance values obtained from the calibration dataset were applied to remove all the values outside this range for both 1991 and 2011. Topographical shadows were removed by applying threshold values to the isolation. A simulated map of direct insolation at acquisition time was used to identify cells with no direct insolation and exclude these from the analysis. Finally, attention was paid to very small changes that can represent a large variation in stock at large scale but that do not represent significant change at the pixel level, using a minimum detectable difference (MDD) approach ([Post et al., 2001](#) and [Garten and Wullschleger, 1999](#)). The MDD is defined as the “smallest difference that can be detected between two mean soil organic carbon inventories with a certain level of confidence given the average variance and sample size”. Considering that the sample size in our study was the number of cells (5.3 million for the study area), the formula used by the authors would produce a very low MDD, and so this approach was modified. MDD was defined here, for each cell, as the maximum standard deviation of either $SOC_{sd-2011}$ or $SOC_{sd-1991}$. If the absolute soil carbon change

($SOC_{1991-2011}$) was below the MDD, no change was assumed (zero value).

3. Results

3.1. SOC stock plot dataset

In the dry region, the SOC stocks ranged from 38 to 72 MgCha⁻¹ for the 30 cm soil layer, and 81–141 MgC.ha⁻¹ for the 100 cm soil layer. In the humid region, the range was 70–131 MgC.ha⁻¹ for the 30 cm soil layer and 139–296 MgC.ha⁻¹ for the 100 cm soil layer. The coefficient of variation was slightly higher for the 30 cm soil layer (39%) than for the 100 cm soil layer (31%). Overall, the SOC in the 30 cm soil layer accounted for half (49%) of the SOC stored in the 0–100 cm soil layer. There were also considerable differences in the SOC content and rock fragment content between these two regions.

3.2. Model accuracy assessment

We obtained R^2 of 0.72 for the 0–30 cm soil layer and 0.69 for the 0–100 cm soil layer ([Table 3](#)). RMSE were 14 and 23 MgC.ha⁻¹ representing 27% and 23% of the mean. R^2 ranged from 0.49 to 0.91 for the 0–30 cm soil layer and 0.43 to 0.88 for the 0–100 cm soil layer. This slight reduction in performance with depth is not surprising and confirmed previous reports ([Malone et al., 2009](#)). Reasons may be the use of a pedotransfer function (splines) to estimate soil properties (bulk density, carbon content, rock fragment) along the 0–100 cm soil profile and the lack of predictors for soil properties below ground. Despite clear underestimation of high SOC values for some validation points ([Fig. 2a](#)), the overall model shows only a slight bias (0.5 and 0.3 MgC.ha⁻¹).

3.3. Importance of soil carbon controlling factors

The importance of each variable was studied i) by analysing pair-wise correlation of SOC stocks with the covariates and ii) by analysing the internal randomForest variable importance metric.

Pair-wise correlation between SOC stocks and spatial covariates showed interesting patterns ([Table 2](#)). Nine of the twenty spatial covariates had correlation (r) values above 0.3, including visible and mid infra-red bands (1,2,3,5,7), valley depth and the two climatic variables (precipitation and temperature). Near infra-red was weakly correlated with SOC stocks (0.07), and the thorium relative concentration was relatively high (0.20) for the top soil layer. Similar trends were observed for both the 0–30 cm and 0–100 cm soil layers, with almost systematically lower correlations for the 0–100 cm soil layer.

The relative importance of the soil-landscape factors was further analyzed by calculating the *NodePurity* index ([Fig. 2b](#)). Again, similar patterns were found for both soil layers. Precipitation and temperature both explain regional SOC patterns to a far greater extent than other factors. The factors obtained from gamma radiometry, especially thorium surface concentration, appeared to have a significant influence on SOC distribution. Finally, with similar relative importance, the visible (bands 1 and 3) and mid infra-red (band 7) reflectance and some topographic variables (valley height, altitude) stand out from the other factors. The SOC 30 and 100 models differ with temperature being less important and thorium being more important for the 0–100 cm soil layer.

3.4. Spatio-temporal estimates of SOC stocks

The prediction of SOC stocks in the 0–30 and 0–100 cm soil layers, at a 30 m resolution over the entire study area for 1991 and 2011, is shown in [Fig. 3](#).

Table 3

Averaged validation indices for the 10 cross-validation runs. Minimum and maximum values recorded are in brackets.

Soil layer (cm)	R ²	RMSE (MgCha ⁻¹)	RMSE (%)	Bias (MgCha ⁻¹)	RPD
0–30	0.72 [0.46, 0.91]	14.4 [9.5, 18.3]	26 [18, 34]	0.5 [−4.7, 2.9]	1.97 [1.38, 3]
0–100	0.69 [0.43, 0.88]	23.5 [17.6, 31.5]	22 [17, 27]	0.3 [−8.5, 7.8]	1.88 [1.34, 2.5]

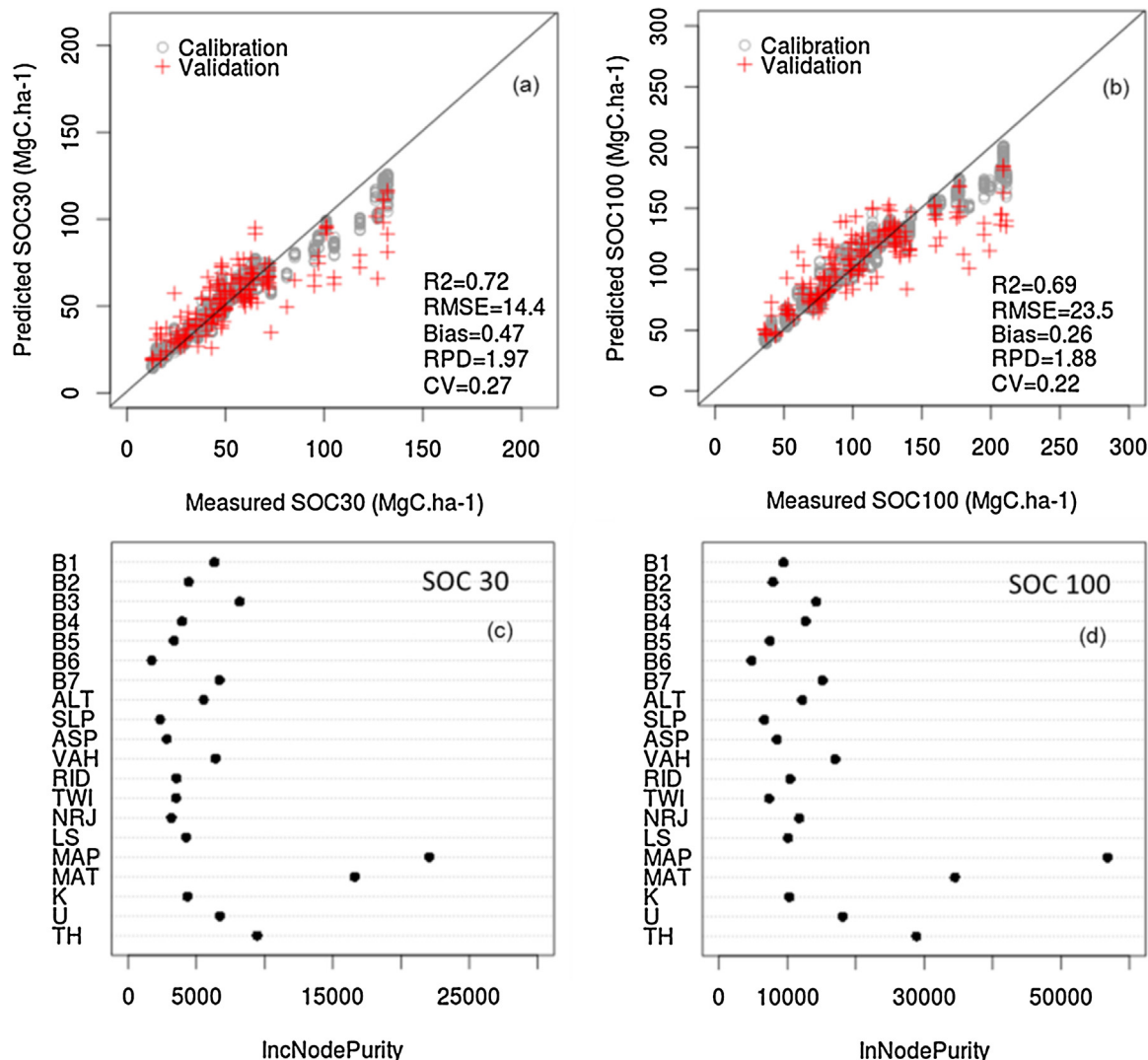


Fig. 2. Predicted vs Measured plot for calibration and validation datasets for SOC 0–30 cm soil layer (a) and 0–100 cm (b) soil layer and average relative importance of variables for both spatial models (c and d). Variable names and description are given in Table 2. The accuracy measurements (R², RMSE, Bias, RPD, CV) are those calculated for the validation dataset (see also Table 3).

Post processing steps to remove topographic shadows and out-of-reflectance-range pixels reduced the study area from 474,661 ha to 351,117 ha for the 2011 map and 256,000 ha for the 1991 map. Shadows accounted for 40,467 ha (8.5%) and out-of-reflectance-range pixels accounted for 83,077 ha (17.5%) for 2011 and 178,194 ha (37.5%) for 1991. The areas eliminated were mainly in areas with steep slopes in both the dry and humid regions. The northern part of the study area, wetlands (not sampled) and some densely forested areas were excluded as the soil and vegetation conditions were different from the reference area. The small amount of cloud cover was also removed during post processing.

The SOC stock maps produced clear patterns. Firstly, an east–west gradient from high to low SOC stock is visible, influenced by the precipitation gradient. Secondly, the temperature and altitude, which are highly correlated factors ($r=0.89$), are also responsible for great variations, with low stocks in low altitude, warmer regions and higher stocks in high altitude, cooler regions. Thirdly, the land cover and topographical effects on SOC change are less pronounced within the landscape. Nevertheless, changes can be seen on the edge of the tropical humid forest as well as in cultivated plots on the slopes (enlargement in Fig. 3). Generally, both 1991 and 2011 maps show the same overall pattern (Fig. 3 and Table 4). We observed an average of 25 MgCha⁻¹ difference between forest and

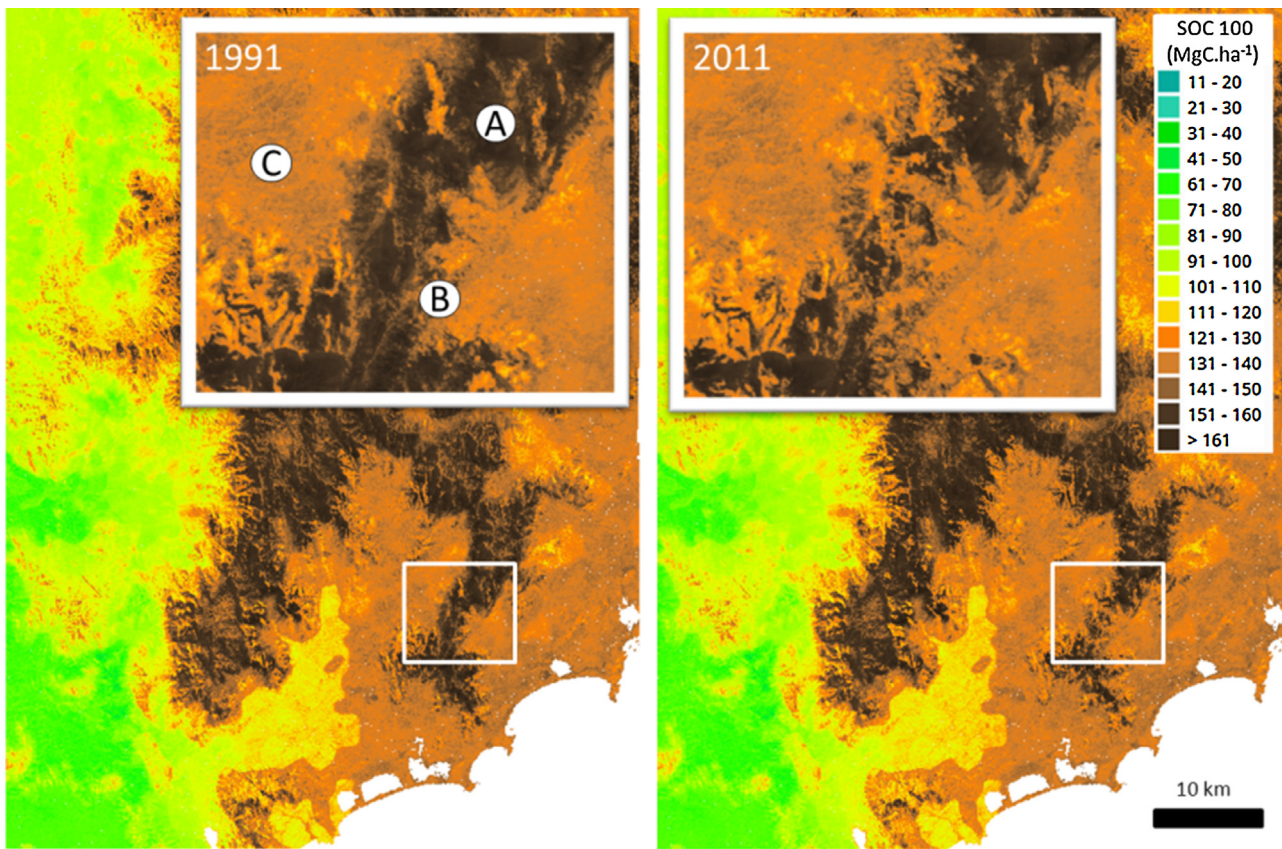


Fig. 3. SOC (0–100 cm) maps produced for 1991 and 2011 for the entire study area and an enlargement of a mountainous and forested landscape (A) associated with shifting cultivation plots (B) and undulating grassland valley (C).

Table 4

Estimated SOC stocks for forest and crop/savannah land cover for the 0–30 cm and 0–100 cm soil layers taken from 1991 and 2011 carbon maps.

Climatic region	Land cover (2010)	Area (ha)	SOC stock 1991 (MgC.ha ⁻¹)				SOC stock 2011 (MgC.ha ⁻¹)			
			30 cm		100 cm		30 cm		100 cm	
			mean	s.d.	mean	s.d.	mean	s.d.	mean	s.d.
Humid	Forest	116 998	83.2	11.5	145.1	12.4	87.0	10.4	146.3	11.6
	Crop and savannah	194 162	61.0	7.2	125.5	10.1	61.0	7.0	125.4	9.7
Dry	Forest	766	39.4	9.4	83.1	14.7	40.1	9.7	84.2	15.3
	Crop and savannah	93 493	45.2	10.7	92.2	16.3	46.8	10.5	94.7	16.3

crop/savannah in the humid area (87.4 and 61.4 MgC.ha⁻¹ respectively in 2011). Carbon stocks were estimated to be 5–7 MgC.ha⁻¹ lower in forests than in crop/savannah in dry regions, but this difference was of the same order of magnitude of the standard deviation (10 MgC.ha⁻¹).

3.5. Detecting changes in SOC stocks at regional scale

Applying the MDD threshold to the SOC change maps identified 47,287 ha (10%) with significant SOC changes for 0–30 cm soil layer, and 38,376 ha (8.1%) for the 0–100 cm soil layer. The remaining areas of 173,248 ha (36.4%) and 182,159 ha (38.3%) was set to zero change (no significant changes). This map is shown in Fig. 4.

In the humid region, there was a large area with significant potential soil carbon loss around the forest edges, in known deforestation areas (see Section 3.6) as well as outside known deforestation areas. For the 0–30 cm soil layer, the largest reduction in stocks (1991) was 40.8% and the largest increase was 58.3%. The 1% and 99% quantiles were at −23% and +13% (Table 5).

In the dry region, for the 0–30 cm soil layer, the largest reduction in stocks was 42.1% and largest increase was 83.4%, and the 1% and 99% quantiles were at −12.9% and +15.4%. The changes in SOC for the 0–100 cm soil layer were always lower than for the 0–30 cm soil layer, from approximately −12% to +12% for both regions (1% and 99% quantiles).

At the landscape scale, in the humid region, there was a significant increase in SOC stocks in forested areas and in small patches of the valleys and downhill slopes. In the dry region, the SOC distribution patterns are less clear with generally a small increase in stocks and some distinct major reductions. There was no particular trend in grassland areas. The three dimensional view (Fig. 4) highlights the locations of the changes in SOC stocks within the landscape. A mosaic of cropland and fallow (shifting cultivation) on the slopes was particularly subject to reduction in SOC stocks of more than 10% in 20 years. Larger reductions (between 15% and 40%) could be seen in the middle to top slopes, reductions of around 10% could be seen downhill but there were no reductions in the valleys. SOC stocks increased in other small areas of land spread over the hills and in the valleys.

SOC stock change (1991–2011)

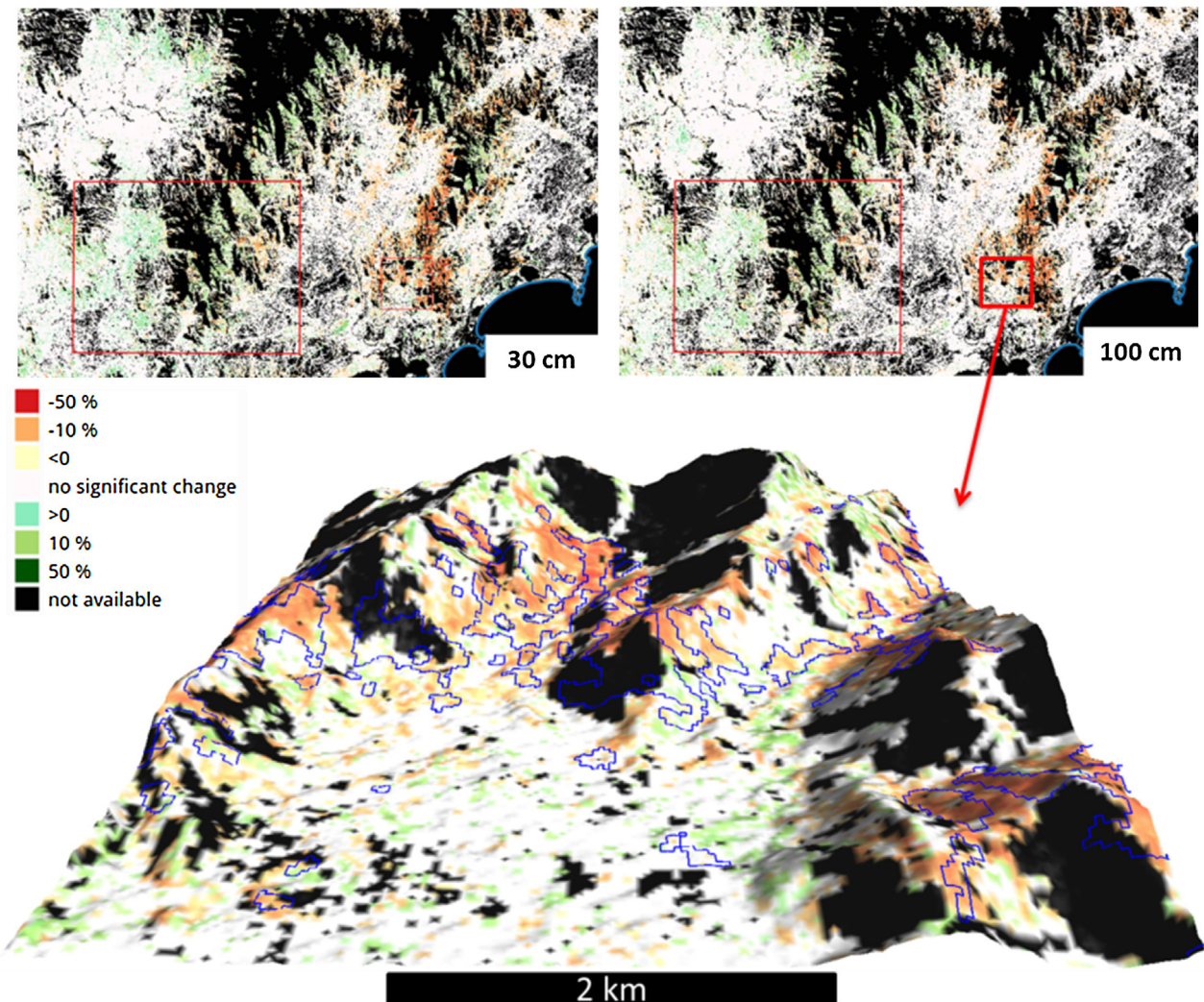


Fig. 4. Potential SOC change map 1991–2011 for the 0–30 cm and 0–100 cm soil layers and a 3D landscape view. The area in white represents no significant change and no data is available for the areas in black. The blue polyline encloses the areas subject to deforestation between 1990 and 2010 (MEFT, 2009; Grinand et al., 2013). (For interpretation of the references to colour in this figure legend, the reader is referred to the web version of this article.)

Table 5

Potential changes in SOC stocks over the study area. “n” is the number of observations/pixels.

Climate region	Soil layer (cm)	n	SOC stock change (%) quantile values								
			Min	1%	5%	25%	50%	75%	95%	99%	Max
Humid	0–30	1 473 532	−40.8	−23.1	−11.8	0	0	0	6.4	13.7	58.3
	0–100	1 473 532	−28.4	−12.6	−6.3	0	0	0	3.6	7.8	33.3
Dry	0–30	970 710	−42.1	−12.9	0	0	0	0	6.0	15.4	83.4
	0–100	970 710	−28.4	−7.9	−2.9	0	0	0	4.6	12.4	36.6

Analyzing the correlation between the changes in SOC stocks and the initial stocks (Fig. 5) showed that the highest potential reduction in the humid region was correlated with the highest initial SOC stocks. The highest potential increase was for areas with average stocks. In the dry region, the trends were similar, but less pronounced. The highest potential increase, however, appeared to be for the lowest initial SOC stocks.

3.6. Changes in SOC stocks in deforested areas

SOC stocks change maps were compared with already published maps that located deforestation for three periods: 1990–2000,

2000–2005 and 2005–2010 (MEFT, 2009; Grinand et al., 2013). The analysis was based on 8326 and 50,399 cells in the dry and humid regions respectively (Table 6). In the humid region, the change in SOC for deforested areas was −10.7% for the 0–30 cm and −5.2% for the 0–100 cm soil layer. In the dry region, the net change of SOC in deforested areas was close to zero (−0.1%, −0.33%) for the 0–30 cm and 0–100 cm soil layers respectively.

The changes in SOC for areas deforested over three periods (1990–2000, 2000–2005, 2005–2010) were calculated only for the 0–30 cm layer (Fig. 6). The average potential reductions were 9.6%, 10.7% and 11.7% respectively in each of these deforestation periods.

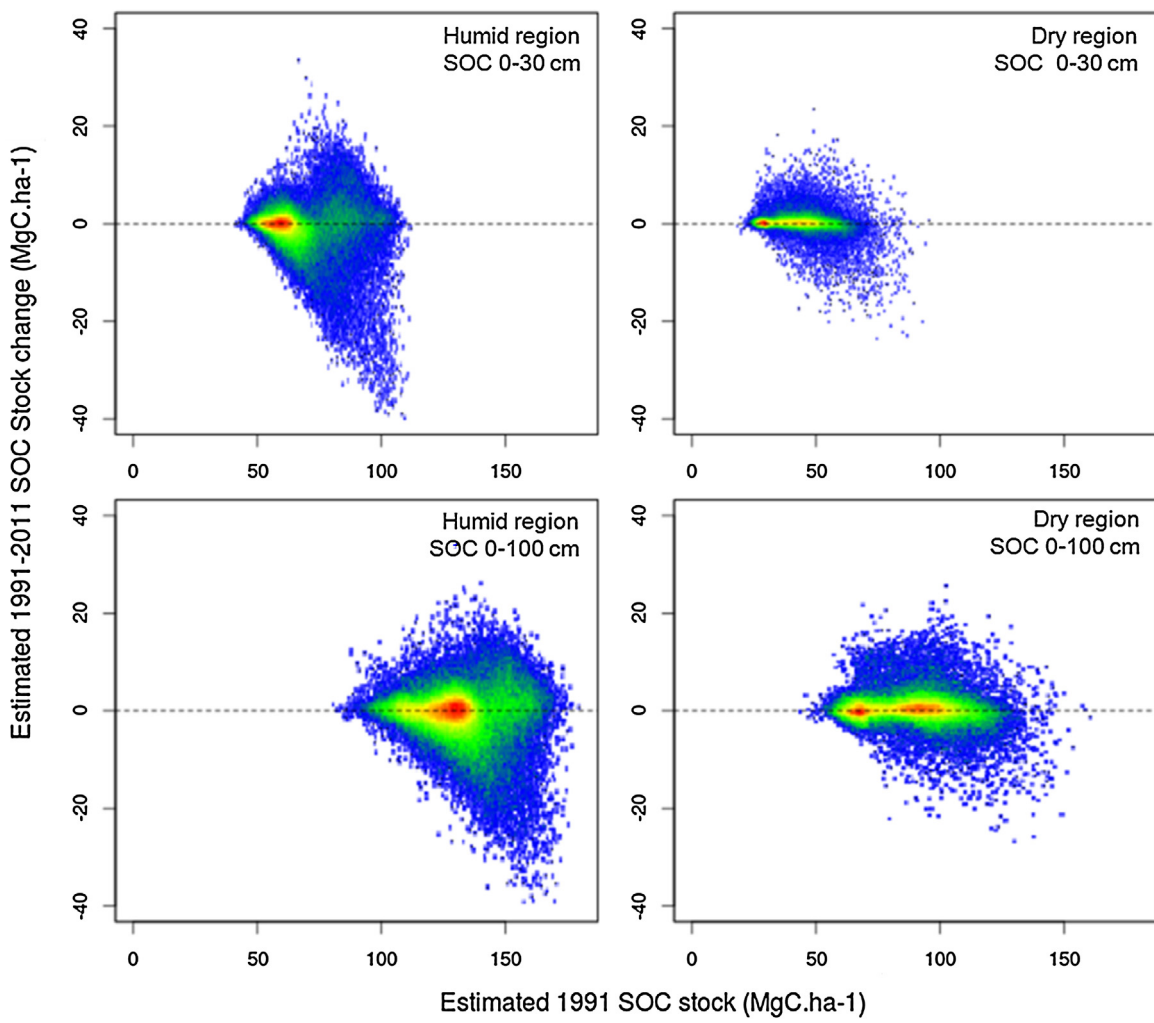


Fig. 5. Potential changes in SOC stocks estimated as a function of the initial stocks over the study area. Each graph were created using 100 000 observations/pixels randomly selected. Colors indicate density of observations/pixels (from white-blue to green, red). (For interpretation of the references to colour in this figure legend, the reader is referred to the web version of this article.)

Table 6
Changes in SOC stocks for areas deforest in various periods. “n” is the number of SOC change observations (pixels). 5%q and 95%q are the 5% and 95% quantiles. S.D. is the standard deviation.

Climatic region	Soil layer (cm)	Period of forest to cropland conversion	n	Absolute change of SOC (MgC.ha^{-1})				Relative change of SOC (%)				Average stock prior to conversion (MgC.ha^{-1})
				Mean	S.D.	5%q	95%q	Mean	S.D.	5%q	95%q	
Dry	0–30	1990–2010	8 326	-0.2	2.0	-3.5	2.1	-0.1	3.8	-6.3	5.3	38.9
	0–100	1990–2010	8 326	-0.3	2.7	-4.2	4.0	-0.3	2.9	-4.9	4.7	83.2
Humid	0–30	1990–2010	50 399	-8.8	9.0	-27.0	0.0	-10.7	9.9	-29.1	0.0	75.7
	0–100	1990–2010	50 399	-7.6	8.9	-25.0	0.0	-5.2	5.9	-16.3	0.0	140.3

4. Discussion

4.1. How are the SOC stocks distributed and what are the underlying drivers?

First, at plot scale and for the 0–30 cm soil layer, we recorded an average of 69.2 MgC.ha^{-1} and 38 MgC.ha^{-1} . These figures are similar to those estimated by Grinand et al. (2009) for the two dominant soils in Madagascar: the Ferralsol (61.3 MgC.ha^{-1}) and Oxisol (33.6 MgC.ha^{-1}). These observations reflect the discrepancies in dominant soil types found in the two ecoregions (see Section

2.1) and ecological processes (less primary biomass productivity inputs and increasing mineralization with increasing temperature in the dry region).

Then, the regression quality indices of the soil-landscape model (R^2 of 0.72 and 0.69) were comparable with other regional and fine-scale studies. Adhikari et al. (2014) reported R^2 values ranging from 0.23 to 0.63 in Denmark, Malone et al. (2009) reported R^2 of 0.44 in Australia, Vagen and Winowiecki (2013) reported R^2 of 0.65 in Ethiopia and Wiesmeier et al. (2011) reported R^2 of 0.74 in China. The slight underestimation of high SOC values may be explained by an under representation of these values in the training

SOC stock change (0–30 cm – humid region) between 1991 and 2011 for various deforestation periods

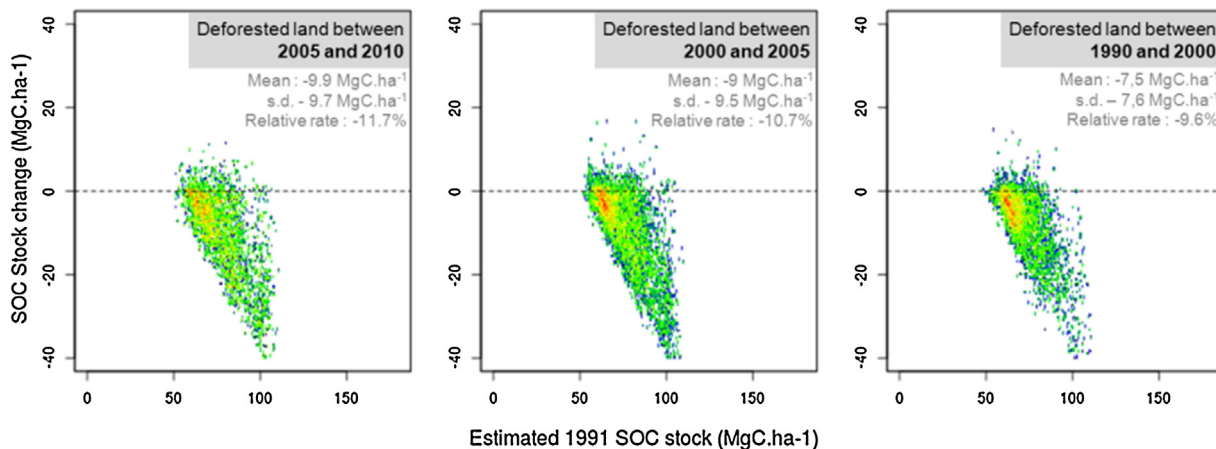


Fig. 6. SOC change (0–30 cm – humid region) between 1991 and 2011 for various deforestation periods. Each graph were created using 15 000 observations/pixels randomly selected. Colors indicate density of observations/pixels (from white-blue to green, red). (For interpretation of the references to colour in this figure legend, the reader is referred to the web version of this article.)

dataset. However, this should not affect the estimated changes in SOC stocks as the differences between SOC stocks were computed. The most important explanatory variables in the model underlined the dominant role of climate on SOC distribution. Small changes in future climate trends will have a considerable effect on the storage of soil carbon. This is an important finding for predicting the effect of global changes on future SOC stocks. The role of climate on SOC storage is not yet fully understood, but there is a consensus in the literature that, as total annual rainfall increases, increased biomass production will increase SOC stocks while higher mean annual temperatures may increase mineralisation, thus decreasing SOC stocks (Chaplot et al., 2010). However, laboratory experiments do not always confirm this increased SOC turnover (Hamdi et al., 2013).

Secondly, gamma radiometry, used as a proxy of the parental material, was an unexpectedly important predictor of SOC stocks. The literature has shown gamma radiometry to be a proxy of water retention and clay content (Rawlins et al., 2009) and more generally for characterising erosion, deposition and weathering processes (Wilford and Minty, 2006). However, one of the very few studies on soil carbon mapping using gamma radiometry reported that, of the three elements, K was the most important (Malone et al., 2009). So far as we are aware, no studies have been carried out on Th as a strong predictor of SOC stocks. Wilford and Minty (2006) explained that Th and U are associated with more stable weathered constituents in the soil profile unlike K which is easily displaced during weathering and leaching. Besides, during weathering, Th and U are “readily absorbed onto clay minerals, oxides (Fe and Al) and organic matter” which may explain the high importance of Th in our model. This is a significant finding as Madagascar has a high coverage of gamma radiometry images which may considerably improve soil inventories or mapping programs.

Thirdly, soil-vegetation and topographic factors are significantly correlated with SOC but to a lesser extent in the model. The magnitude of spatial variation of those factors at local scale is high which explain a more complex and not homogeneous relationship over the study area.

4.2. Can significant changes in SOC stocks be detected using satellite images?

This study explored the use of archive satellite images to estimate changes in SOC stocks at fine scale within a region. The results

show a wide range of changes, between approximately -40% to +40% of the initial stocks (Table 5) over a twenty year period. The approach is empirical based on two points in time and was referred to as *potential change* since the soils at the two dates cannot be considered to be at equilibrium. This raises the question of whether this approach is competitive with other well-known techniques and whether the results are accurate.

The spatio-temporal extrapolation issues are addressed by focusing on accuracy, the key aspect being ensuring the validity of the predictions. The post-processing controls reduced the area under investigation by about half, especially far from the reference area. This was to be expected as the soil conditions and environment are variable. Topographic shadows covered a significant area as well as zones such as wetland which were not sampled. One way to overcome these limitations and increase the area under study is to increase the number of points sampled. Furthermore, large areas of forest in the 1991 image were removed despite pair-wise reflectance calibration. This may be because the soil moisture or phenology conditions were different from those in the 2011 image. A top-of-the-canopy atmospheric correction may be used. However, there is no unique and robust atmospheric correction and there may still be temporal bias with our methodology, especially in local areas of the image if there are changes in atmospheric conditions within the study area. Setting the change to non-significant value using MDD criteria minimizes small but potentially very wide area changes and improves the statistical strength. The estimated changes in SOC stocks cannot be validated directly since no past data are available. Indirectly, we observed that the average SOC stocks on stable land cover (Table 4) were similar which suggests that there is no obvious bias in our estimates.

Other empirical SOC stock change evaluation methods, such as point sampling based on either chronosequences or time series, suffer from low spatial representativeness over a country, or even over a landscape. They require an extensive soil monitoring system (Morvan et al., 2008) to be set up, which is rarely possible, or would require many years to provide useful and reliable data. Simulating changes in SOC stocks using dynamic models suffers from the same spatial limitations. Our spatial assessments of potential changes in SOC stocks makes it possible to produce thousands or millions georeferenced observations of SOC change (pixels) however, the results suffer from a lack of knowledge on the effects of land use or land management. Hypotheses can be made concerning explanatory factors

that cause changes in SOC stocks but these need to be verified in the field. If they are confirmed, this approach may be adapted to take account of subtle effects that cannot be properly addressed by mechanistic models (e.g. forest degradation, natural regeneration). One way to explain changes in SOC stocks would be to perform inverse modeling, using spatially explicit factors. This study only attempted to analyze the effect of deforestation and initial SOC stocks. This empirical approach is a useful initial and cost-effective method to gain knowledge on historical soil dynamics.

4.3. How are the estimated changes in SOC stocks linked to land cover and changes in land cover?

The maps of changes in SOC stocks in the 0–30 cm and 0–100 cm soil layers were analyzed for various land covers and land cover changes. The differences between forest and crop/savannah stable land cover in the humid region were 20–25 MgC.ha⁻¹ (Table 4). Surprisingly, in the dry region, the average SOC stocks were slightly higher in the crop/savannah areas compared to those estimated in the dry forest. One possible explanation is that the dry area derived from the ecological map include a mix of humid and dry ecophysiological conditions, thus resulting in less distinct pattern in the dry region. Local knowledge would be required to delineate a transition zone between humid and the dry region.

At landscape scale, there are areas of SOC stock reductions for crop/savannah land cover on slopes. These may be associated with crop practices as well as ongoing erosion. There are some stock reductions in forested areas, which may be caused by degradation but this appears to be limited. However, there are large areas of SOC stock increases in forested areas in both humid and dry regions. This may be the result of a reduction in the use of wood products related to security issues over recent years. Small patches of SOC stock increases in the valleys and in the plain may be associated with fallow or plantation. These hypotheses should be confirmed by a detailed survey of historical practices.

In the deforested areas in the humid region, there was an estimated average change in SOC stocks of −10.7% and −5.2% in the 0–30 cm and 0–100 cm soil layers, respectively. These results are consistent with recent meta-analyses. Don et al. (2011), in its meta-analysis of tropical land use change studies, estimated an average relative change of −25.2% for forest converted to cropland, −12.1% for conversion to grassland and −8.6% for conversion to secondary forest. More recently, Powers et al. (2011) estimated changes at −15.4% in average. The rotation cycle and management strategies in this region of Madagascar depend strongly on the requirements of smallholders but are generally 3 years of rainfed rice, 4–6 years of fallow followed by either rice or cassava, and so on. These plots tend to turn to grassland after 10–15 years. The overall trend observed in this study is, therefore, consistent, but slightly lower, than that in the literature, but provides additional spatially explicit information.

This study gave no significant change in SOC stocks for deforestation in the dry region. There are only a few studies for this climate in the literature. Guo and Gifford (2002) carried out a meta-analysis of 18 studies for regions with less than 1000 mm precipitation per year and found that there was a slight reduction in SOC stocks which was significantly different from zero at 95% confidence. Some studies for higher annual precipitation reported an increase in SOC stocks, although it is not clear what could explain such results.

The detailed analysis of SOC change for different periods of deforestation (1990–2000, 2000–2005 and 2005–2010) showed only very low differences. This suggests that the reduction in stocks occurred the first five years after slash and burn practices. Furthermore, the average potential reduction for areas deforested in

1990–2000 (9.6%) was close to the average of all three periods (10.7%), which showed that the recovery of the SOC stocks is low even after 10 years. This is in agreement with Fujisaki et al. (2015) who reported a reduction of 8.5% over 9 years in French Guyana, Brazil, Colombia and Surinam. The slightly higher estimate in this study may be explained by the relatively higher slopes in the study area. The SOC stocks stabilisation or slight recovery after 10 years, may be explained by the crop rotation described above, especially as the land reverts to grassland when it is completely abandoned. Grasslands are known to sequester more carbon in soils than forests (Powers et al., 2011; Fujisaki et al., 2015).

The change in SOC stocks varied considerably, including an increase after deforestation. This has been previously reported (Don et al., 2011) with changes in SOC stocks after deforestation ranging from −80% to +68%. The spatially explicit map of changes in SOC stocks provides a more detailed explanation, in particular concerning the possible role of erosion. There is much discussion about the lateral movement of eroded organic C and its fate within the landscape in agricultural systems: SOC erosion may be a major C source or C sink as SOC translocated by erosion may be buried and protected in hollows or oxidized and emitted (Quinton et al., 2010 in Croft et al., 2012). Locally, SOC stocks after deforestation increased, mainly in the valleys. This may be due to the burial of organic matter as well as rapid regeneration. This hypothesis seems relevant since Chaplot et al. (2005), in a study of hill-slopes in northern Laos, showed that most of the SOC material carried by water erosion (84% of 0.069 kg C m⁻²) accumulated in valley bottoms in areas with steep slopes. Rapid reduction in SOC stocks after deforestation suggests that natural resource managers and policy makers should implement soil conservation measures immediately after the soil has been exposed (Labrière et al., 2015), even though the SOC may later be displaced.

5. Conclusions

This study has proposed a novel approach for estimating potential changes in SOC stocks over a 20 year period without prior information on the soil properties and quantified the effect of deforestation. This landscape scale approach revealed the high variations of SOC stocks with climate and geological basement rock, and lesser variations with topography and soil-vegetation factors. The effect of deforestation was not significant in the dry region (<1000 mm) and an average reduction in SOC stocks of 10.7% was found for the humid region (>1000 mm) area. The largest changes in SOC stocks were in the 0–30 cm soil layer.

However, the direction and magnitude of the change greatly varied at local scale. As clear-cutting forest may increase or reduce SOC stocks depending on the landscape and land management, spatially explicit information on changes in SOC stocks is required to help authorities or NGOs to target sustainable land management actions. It is clear that the higher potential reductions were in soils with high SOC stocks.

Soil carbon change analysis using satellite image shows great potential for evaluating historical changes in regions that do not have a legacy of soil data or monitoring networks. This technique may, therefore, be used as a preliminary approach for evaluating historical trends validated by in-depth social and soil inventories for individual plots. Once validated, the system can provide a cost-effective approach for i) identifying hot spots of changes in stocks and ii) monitoring changes in SOC stocks with limited field data. Building scenarios for future changes would be the next step in developing a decision-making tool including comprehensive information on the actual level of soil degradation or recovery, and the risks and opportunities of various scenarios.

Acknowledgements

This study was partly funded by IRD (Institut de Recherche pour le Développement), Association Etc Terra and the PHCF (Programme Holistique de Conservation des Forêts à Madagascar). The first author was funded by an ANRT PhD scholarship (CIFRE N°2012-1153). The authors thank Tony Tebby for the English revision and the two anonymous reviewers for their helpful comments.

References

- ASTERGDEM, 2011. Global Digital Elevation Model v2. NASA/METI. <http://www.jspacesystems.or.jp/ersdac/GDEM/E/1.html>.
- Adhikari, K., Hartemink, A.E., Minasny, B., Bou Kheir, R., Greve, M.B., Greve, M.H., 2014. Digital mapping of soil organic carbon contents and stocks in Denmark. *PLoS One* 9 (8), e105519, <http://dx.doi.org/10.1371/journal.pone.0105519>.
- Asner, G., Mascaro, J., Muller-Landau, H., Vieilledent, G., Vaudry, R., Rasamoelina, M., Hall, J., van Breugel, M., 2012. A universal airborne LiDAR approach for tropical forest carbon mapping. *Oecologia* 168 (4), 1147–1160.
- Baccini, A., Goetz, S.J., Walker, W.S., Laporte, N.T., Sun, M., Sulla-Menashe, D., Hackler, J., Beck, P.S.A., Dubayah, R., Friedl, M.A., 2012. Estimated carbon dioxide emissions from tropical deforestation improved by carbon-density maps. *Nat. Clim. Change* 2, 182–185.
- Boenntinger, J.L., Howell, D.W., Moore, A.C., Hartemink, A.E., Kienast-Brown, S., 2010. *Digital Soil Mapping, Bridging Research, Environmental Application, and Operation Progress in Soil Science*. Springer (439p).
- Breiman, L., 2001. *Random forests*. *Mach. Learn.* 45, 5–32.
- Casey, R.M., Hill, T., Woollen, E., Ghee, C., Mitchard, E., Cassels, G., Grace, J., Woodhouse, I.H., Williams, M., 2012. Quantifying small-scale deforestation and forest degradation in African woodlands using radar imagery. *Global Change Biol.* 18, 243–257.
- Chaplot, V.A.M., Rumpel, C., Valentim, C., 2005. Water erosion impact on soil and carbon redistributions within uplands of Mekong River. *Global Biogeochem. Cycles* 21 (4), <http://dx.doi.org/10.1029/2005GB002493>.
- Chaplot, V., Bouahom, B., Valentim, C., 2010. Soil organic carbon stocks in Laos: spatial variations and controlling factors. *Global Change Biol.* 16, 1380–1393, <http://dx.doi.org/10.1111/j.1365-2486.2009.02013.x>.
- Costa Jr., C., Corbeels, M., Bernoux, M., et al., 2013. Assessing soil carbon storage rates under no-tillage: comparing the synchronic and diachronic approaches. *Soil Tillage Res.* 134, 207–212, <http://dx.doi.org/10.1016/j.still.2013.08.010>.
- Cowie, A.L., Penman, T.D., Gorissen, L., 2011. Towards sustainable land Management in the drylands: scientific connections in monitoring and assessing dryland degradation, climate change and biodiversity. *Land Degrad. Dev.* 22, 2448–2460.
- Croft, H., Kuhn, N.J., Anderson, K., 2012. On the use of remote sensing techniques for monitoring spatio-temporal soil organic carbon dynamics in agricultural systems. *Catena* 94, 64–74.
- Don, A., Schumacher, J., Freibauer, A., 2011. Impact of tropical land-use change on soil organic carbon stocks—a meta-analysis. *Global Change Biol.* 17, 1658–1670.
- Easter, M., Pausian, K., Killian, K., et al., 2007. The GEFSCOC soil carbon modelling system: a tool for conducting regional-scale soil carbon inventories and assessing the impacts of land use change on soil carbon. *Agric. Ecosyst. Environ.* 122 (1), 13–25, <http://dx.doi.org/10.1016/j.agee.2007.01.004>.
- El Hajj, M., Bégué, A., Lafrance, B., Hagolle, O., Dedieu, G., Rumeau, M., 2008. Relative radiometric normalization and atmospheric correction of a SPOT 5 time series. *Sensors* 8 (4), 2774–2791, <http://dx.doi.org/10.3390/s8042774>.
- Fujisaki, K., Perrin, A.S., Desjardins, T., Bernoux, M., Balbino, L.C., Brossard, M., 2015. From forest to cropland and pasture systems: a critical review of soil organic carbon stocks changes in Amazonia. *Global Change Biol.*, <http://dx.doi.org/10.1111/gcb.12906> (in press).
- Goidts, E., Van Wesemael, B., Crucifix, M., 2009. Magnitude and sources of uncertainties in soil organic carbon (SOC) stock assessments at various scales. *Eur. J. Soil Sci.* 60, 723–739.
- Goodman, S.M., Benstead, J.P., 2005. Updated estimates of biotic diversity and endemism for Madagascar. *Oryx* 39, 73–77.
- Grimm, R., Behrens, T., Marker, M., Elsenbeer, H., 2008. Soil organic carbon concentration and stocks on barro Colorado Island—digital soil mapping using random forest analysis. *Geoderma* 146, 102–113.
- Grinand, C., Rajaonarivo, A., Bernoux, M., Pajot, V., Brossard, M., Razafimbelo, T., Albrecht, A., Le Martret, H., 2009. Estimation des stocks de carbone dans les sols de Madagascar. *Étude et Gestion des Sols* 16 (1), 23–33.
- Grinand, C., Barthès, B.G., Brun, D., Kouakoua, E., Arrouays, D., Jolivet, C., Caria, G., Bernoux, M., 2012. Prediction of soil organic and inorganic carbon contents at a national scale (France) using mid-infrared reflectance spectroscopy (MIRS). *Eur. J. Soil Sci.* 63, 141–151, <http://dx.doi.org/10.1111/j.1365-2389.2012.01429.x>.
- Grinand, C., Rakotomalala, F., Gond, V., Vaudry, R., Bernoux, M., Vieilledent, G., 2013. Estimating deforestation in tropical humid and dry forests in Madagascar from 2000 to 2010 using multi-date Landsat satellite images and the random forests classifier. *Remote Sens. Environ.* 139, 68–80.
- Grunwald, 2009. Multi-criteria characterization of recent digital soil mapping and modeling approaches. *Geoderma* 151, 195–207.
- Guo, L.B., Gifford, R.M., 2002. Soil carbon stocks and land use change: a meta analysis. *Global Change Biol.* 8, 345–360.
- Gutman, G., Byrnes, R., Covington, M.S., Justice, C., Franks, S., Headley, R., 2005. Towards monitoring land-cover and land-use changes at global scale: the global land use survey. *Photogramm. Eng. Remote Sens.* 64, 6–10.
- Hamdi, S., Moyano, F., Sall, S., Bernoux, M., Chevalier, T., 2013. Synthesis analysis of the temperature sensitivity of soil respiration from laboratory studies in relation to incubation methods and soil conditions. *Soil Biol. Biochem.* 58, 115–126.
- Harper, G., Steininger, M.K., Tucker, C.J., Juhn, D., Hawkins, F., 2007. Fifty years of deforestation and forest fragmentation in Madagascar. *Environ. Conserv.* 34, 1–9.
- Hervieu, J., 1960. Notice De La Carte pédologique De Reconnaissance Au 1/200 000ème, Fort-Dauphin, Feuille N° 65. IRSN (51p).
- Hijmans, R.J., Cameron, J.I., Parra, P.G., Jarvis, A., 2005. Very high resolution interpolated climate surfaces for global land areas. *Int. J. Climatol.* 25, 1965–1978.
- Hijmans, R.J., Etten, J.V., Mattiuzzi, M., Sumner, M., Greeberg, J.A., Perpinan Lamigueiro, O., Bevan, A., Racine, E.B., Shortridge, A., 2015. Reading, writing, manipulating, analyzing and modeling of gridded spatial data. version: 2. 3–40, date: 2015-4-10.
- IEFN, 1999. *Carte d'Inventaire Ecologique Et Floristique National. République de Madagascar*, Madagascar.
- IPCC, 2006. *IPCC Guidelines for National Greenhouse Gas Inventories*. IGES, Japan (www.ipcc-nccc.iges.or.jp/public/2006gl/index.html).
- Labrière, N., Locatelli, B., Laumonier, Y., Freycon, V., 2015. Soil erosion in the humid tropics: a systematic quantitative review. *Agric. Ecosyst. Environ.* 203, 127–139.
- Lagacherie, P., Robbez-Masson, J.M., Nguyen-The, N., Barthes, J.P., 2001. Mapping of reference area representativity using a mathematical soilscape distance. *Geoderma* 101, 105–118.
- Lal, R., 2008. The urgency of conserving soil and water to address 21st century issues including global warming. *J. Soil Water Conserv.* 63, 140–141.
- Le Maire, G., Marsden, C., Nouvellon, Y., Grinand, C., Hakamada, J.S., Laclau, J.P., 2011a. MODIS NDVI time-series allow the monitoring of Eucalyptus plantation biomass. *Remote Sens. Environ.* 115 (10), 2624–2625.
- Le Maire, G., Marsden, C., Verhoef, W., Ponzoni, F.J., Lo Seen, D., Bégué, A., Stape, J.L., Nouvellon, Y., 2011b. Leaf area index estimation with MODIS reflectance time series and model inversion during full rotations of Eucalyptus plantations. *Remote Sens. Environ.* 115, 586–599.
- Liaw, A., Wiener, M., 2014. Breiman and Cutler's random forests for classification and regression: Classification and regression based on a forest of trees using random inputs. version: 4. 6–10, date: 2014-07-17.
- MEFT, 2009. Ministry of the environment, forest and tourism of Madagascar. In: *Evolution De La Couverture De Forêts Naturelles à Madagascar*. Antananarivo, Madagascar, 1990–2000–2005, pp 132.
- Malone, B.P., McBratney, A.B., Minasny, B., Laslett, G.M., 2009. Mapping continuous depth functions of soil carbon storage and available water capacity. *Geoderma* 154, 138–152.
- McBratney, A.B., Mendonça, M.L., Minasny, B., 2003. On digital soil mapping. *Geoderma* 117, 3–52.
- McCarty, G., Reeves, J., Reeves, V., Follett, R., Kimble, J., 2002. Mid-infrared and near-infrared diffuse reflectance spectroscopy for soil carbon measurement. *Soil Sci. Soc. Am. J.* 66, 640–646.
- Milne, E., Al-Adamat, R., Batjes, N.H., et al., 2007. National and sub national assessments of soil organic carbon stocks and changes: the GEFSCOC modelling system. *Agric. Ecosyst. Environ.* 122 (1), 3–12, <http://dx.doi.org/10.1016/j.agee.2007.01.002>.
- Milne, E., Banwart, S.A., Noelle-meyer, E., et al., 2014. Soil carbon, multiple benefits. *Environ. Dev.*, <http://dx.doi.org/10.1016/j.envdev.2014.11.005>.
- Minasny, B., McBratney, A.B., Malone, B.P., Wheeler, I., 2013. Digital soil mapping of soil carbon. *Adv. Agron.* 118, <http://dx.doi.org/10.1016/B978-0-12-405942-9.00001-3>.
- Morvan, X., Saby, N.P.A., Arrouays, D., 2008. Soil monitoring in Europe: a review of existing systems and requirements for harmonisation. *Sci. Total Environ.* 391, 1–12.
- Mulder, V.L., de Bruin, S., Schaeppman, M.E., Mayr, T.R., 2011. The use of remote sensing in soil and terrain mapping—a review. *Geoderma* 162, 1–19.
- Phachomphon, K., Dlamini, P., Chaplot, V., 2010. Estimating carbon stocks at a regional level using soil information and easily accessible auxiliary variables. *Geoderma* 155, 372–380.
- Post, W.M., Izaurralde, R.C., Mann, L.K., Bliss, N., 2001. Monitoring and Verifying changes of organic carbon in soil. *Clim. Change* 51, 73–99.
- Powers, J.S., Corre, M.D., Twine, T.E., Veldkamp, E., 2011. Geographic bias of field observations of soil carbon stocks with tropical land-use changes precludes spatial extrapolation. *PNAS* 108 (15), 6318–6322.
- Quinton, N., Govers, G., Van Oost, K.V., Bardgett, R.D., 2010. The impact of agricultural soil erosion on biogeochemical cycling. *Nature Geosci.* 3, 311–314, <http://dx.doi.org/10.1038/ngeo838>.
- R Development Core Team, 2005. *R: A Language and Environment for Statistical Computing*. R Foundation for Statistical Computing, Vienna, Austria (ISBN 3-900051-07-0, URL <http://www.R-project.org>).
- Rabenarivo, M., Chapuis-Lardy, L., Brunet, D., Chotte, J.L., Rabeharisoa, L., Barthès, B.G., 2013. Comparing near and mid-infrared reflectance spectroscopy for determining properties of Malagasy soils, using global or LOCAL calibration. *J. Near Infrared Spectrosc.* 21, 495–509.

- Rawlins, B.G., Marchant, B.P., Smyth, D., Scheib, C., Lark, R.M., Jordan, C., 2009. Airborne radiometric survey data and a DTM as covariates for regional scale mapping of soil organic carbon across Northern Ireland. *Eur. J. Soil Sci.* 60, 44–54.
- Razafimbelo, T., Albrecht, A., Feller, C., 2010. Stockage de carbone dans les sols sous systèmes de culture en semis direct sous couvert végétal (SCV) dans différents contextes pédoclimatiques à Madagascar. *Etude et Gestion des sols* 17, 139–154.
- Razakamanarivo, R.H., Grinand, C., Razafindrakoto, M.A., Bernoux, M., Albrecht, A., 2011. Mapping organic carbon stocks in eucalyptus plantations of the central highlands of Madagascar: a multiple regression approach. *Geoderma* 162, 335–346.
- Sreenivas, K., Sujatha, G., Sudhir, K., Vamsi Kiran, D., Fyzee, M.A., Raviskar, T., Dadhwal, V.K., 2014. Spatial assessment of soil organic carbon density through random forests based imputation. *J. Indian Soc. Remote Sens.*, <http://dx.doi.org/10.1007/s12524-013-0332-x>.
- Shepherd, K.D., Walsh, M.G., 2002. Development of reflectance spectral libraries for characterization of soil properties. *Soil Sci. Soc. Am. J.* 66 (3), 988–998.
- Smith, P., Davies, C.A., Ogle, S., et al., 2012. Towards an integrated global framework to assess the impacts of land use and management change on soil carbon: current capability and future vision. *Global Change Biol.* 18, 2089–2101, <http://dx.doi.org/10.1111/j.1365-2486.2012.02689.x>.
- Vagen, T.G., Winowiecki, L.A., 2013. Mapping of soil organic carbon stocks for spatially explicit assessments of climate change mitigation potential. *Environ. Res. Lett.* 8, 1–9, <http://dx.doi.org/10.1088/1748-9326/8/1/015011>.
- Vagen, T.G., Andrianorofanomezana, M.A.A., Andrianorofanomezana, S., 2006. Deforestation and cultivation effects on characteristics of oxisols in the highlands of Madagascar. *Geoderma* 131, 190–200.
- Vieilledent, G., Grinand, C., Vaudry, R., 2013. Forecasting deforestation and carbon emissions in tropical developing countries facing demographic expansion: a case study in Madagascar. *Ecol. Evol.* 3 (6), 1702–1716, <http://dx.doi.org/10.1002/ece3.550>.
- Vieilledent, G., Gardi, O., Grinand, C., Burren, C., Andriamananjato, M., Camara, C., Gardner, C.J., Glass, L., Rasolohery, A., Rakoto Ratsimbazafy, H., Gond, V., Rakotoarijaona, J.R., 2016. Bioclimatic envelope models predict a decrease in tropical forest carbon stocks with climate change in Madagascar. *J. Ecol.* 104, 703–715.
- Viscarra Rossel, R.A., Walvoort, D.J.J., McBratney, A.B., Janick, L.J., Skjemstad, J.O., 2006. Visible, near infrared, mid infrared or combined diffuse reflectance spectroscopy for simultaneous assessment of various soil properties. *Geoderma* 131, 59–75.
- Wiesmeier, M., Barthold, F., Blank, B., Kögel-Knabner, I., 2011. Digital mapping of soil organic matter stocks using Random Forest modeling in a semi-arid steppe ecosystem. *Plant Soil* 340, 7–24, <http://dx.doi.org/10.1007/s11104-010-0425-z>.
- Wilford, J., Minty, B., 2006. The use of airborne gamma-ray imagery for mapping soils and understanding landscape processes. Chapter 16 in *Digital Soil Mapping – An Introductory Perspective*, Hartemink A.E., McBratney, A., volume 31, pp 207–218, 609–610.